*Journal of Engineering Mathematics* **29:** 575–589, 1995.


# Wave scattering by circular arc shaped plates

M. MCIVER and U. URKA
*Department of Mathematical Sciences, Loughborough University of Technology, Loughborough, Leicestershire, LE11 3TU, UK, email: M.McIver@lut.ac.uk*

Received 2 September 1994, accepted in revised form 3 May 1995

**Abstract.** This work investigates the reflection and transmission properties of a circular arc plate which is submerged in deep water. The purpose is to compare the reflective properties of a circular arc plate with those for a submerged, circular cylinder in order to assess the suitability of using circular arc plates when constructing a water wave lens. Linear theory is assumed and two separate techniques are used to determine the wave field. The first involves expanding the potential as a series of multipole potentials outside a circular region and a series of nonsingular solutions of Laplace's equation within the region and matching the expansions on the boundary. The second technique is based on a variational procedure and is used to derive an explicit, approximate expression for the reflection coefficient, under the assumption that the plate is short compared with the other length scales in the problem. Results are presented which compare the approximate solution with the full numerical method for a variety of plates. Finally, the full numerical calculations of the reflection and transmission coefficients for a plate are compared with those for a submerged, circular cylinder.

## 1. Introduction

The idea of constructing a water wave lens which would focus waves prior to extracting energy from them has been developed by Mehlum & Stamnes [1] and more recently by Murashige & Kinoshita [2]. A lens is constructed from a system of underwater structures which is designed so that a diverging wave experiences a nonuniform phase shift as it passes over the lens which transforms it into a converging wave. Each of the elements of the lens should therefore have the property that it reflects very little of the incoming wave but is able to induce a phase lag in the transmitted wave. Mehlum & Stamnes [3] considered the use of a submerged, circular cylinder as a lens element as Dean [4] had previously shown that this body has the ideal property that it does not reflect normally incident waves of any frequency when placed in water of infinite depth. However, it may not always be possible to construct a cylinder of sufficient size to obtain the phase shifts required and so other bodies have been considered such as submerged, horizontal plates (McIver [5]), chevron shaped plates and arrays of submerged, circular cylinders (Murashige & Kinoshita [2]). Unfortunately however, the simplest of these bodies, the horizontal plate, can reflect quite large amounts of the incident wave over a range of frequencies. The purpose of this work is to investigate the reflection and transmission properties of a circular arc shaped plate. Although it is a plate, this body is shaped like the top of a circular cylinder and so might be expected to have similar reflective properties to the cylinder.

Wave scattering by two-dimensional, flat plates has been considered by many authors. In particular Ursell [6] showed that there is an explicit solution for wave scattering by a surface-piercing vertical barrier in infinite depth water. His work was extended by John [7] to consider barriers inclined at angles $\pi/2n$ to the horizontal, although the solution rapidly becomes more complicated as $n$ increases. Further extensions to submerged plates, obliquely incident waves and more than one barrier have been made by Evans [8], Evans & Morris [9]

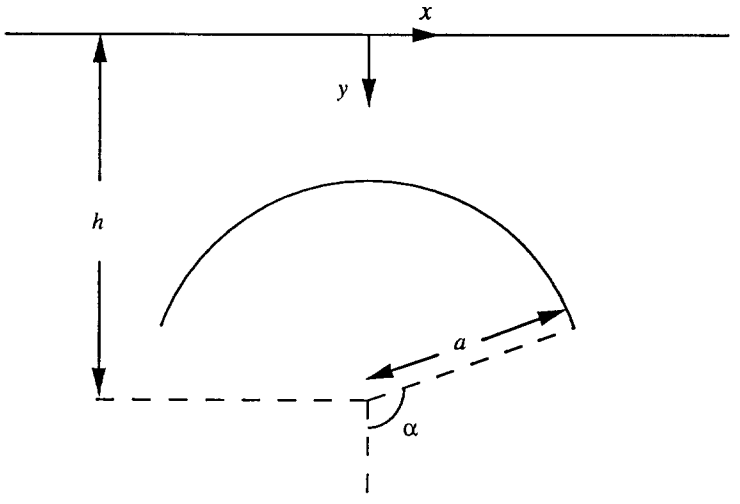


*Fig. 1.* Definition sketch

and Porter [10]. Similarly, the horizontal plate has been the subject of many investigations. Although there does not exist an explicit solution for a finite, horizontal plate, numerical methods such as the finite element method (Patarapanich [11]) and a matched eigenfunction expansion (McIver [5]) have been used to obtain values for the reflection and transmission coefficients. In addition, the Wiener-Hopf technique has been used by Burke [12] and Heins [13] to generate explicit forms for the reflection coefficient associated with a semi-infinite plates, both submerged and in the free surface. More recently, Parsons & Martin [14] have developed a method based on hypersingular integral equations to calculate the reflection from a plate of arbitrary inclination. Their method may be generalised to plates which are not flat and Parsons & Martin [15] presents some results for a submerged, circular arc plate which have been used to verify the results obtained in this work.

Two methods are used here to investigate the reflective properties of a submerged, circular arc plate. The first is based on the method of matched eigenfunction expansions, (see e.g. Mei & Black [17]), and uses the multipole potentials derived by Ursell [16]. In a different physical context, Norris & Yang [18] used a similar technique to calculate the stress on a partially bonded fiber. The second method employs the Schwinger variational approximation, (see e.g. Miles [19]), and explicitly includes the form of the singularity in the velocity at the plate tips in the representation of the potential. These methods are described in §2 and §3 respectively and results are presented in §4.

## 2. The method of matched series expansions

A wave is normally incident from the left on a symmetric, circular arc plate which is submerged in water of infinite depth, as illustrated in figure 1. Cartesian axes are chosen so that the $y$ axis is directed vertically downwards and the $x$ axis lies in the undisturbed free surface. The plate occupies an arc of a circle of radius $a$ with centre at depth $h$. Polar coordinates $(r, \theta)$ based on the centre of the circle are defined such that

$$x = r\sin\theta, \quad y = h + r\cos\theta. \tag{1}$$

The ends of the plate are given by $\theta = \pm\alpha$.

The water is assumed to be inviscid and incompressible and the flow is irrotational and so it may be described by a velocity potential $Re[-igA\phi(x,y)e^{-i\omega t}/\omega]$ where $\omega$ is the frequency of the incoming wave, $A$ is its amplitude and $g$ is the acceleration due to gravity. The wave steepness is assumed to be small and linear theory is used. Thus $\phi$ satisfies

$$\nabla^2\phi = 0 \quad \text{in the fluid} \tag{2}$$

with the free surface boundary condition

$$K\phi + \frac{\partial\phi}{\partial y} = 0 \quad \text{on } y = 0 \tag{3}$$

where $K = \omega^2/g$. The arc is assumed to be fixed and so

$$\frac{\partial\phi}{\partial r} = 0 \quad \text{on } r = a,\ \alpha < \theta < 2\pi - \alpha. \tag{4}$$

At the ends of the plate there will be square root singularities in the velocity. There is no motion at large depths and so

$$\nabla\phi \to 0 \quad \text{as } y \to \infty. \tag{5}$$

The radiation condition at large distances may be expressed as

$$\phi \sim \begin{cases} e^{iKx-Ky} + Re^{-iKx-Ky} & \text{as } x \to -\infty \\ Te^{iKx-Ky} & \text{as } x \to \infty. \end{cases} \tag{6}$$

where $R$ and $T$ are the reflection and transmission coefficients respectively.

A representation for $\phi$ is obtained by splitting the fluid into two regions, namely the inside and outside of the circle of radius $a$. In the outer region the potential may be considered to arise from a certain normal velocity distribution around the circle and so may be expressed in terms of the multipole potentials derived by Ursell [16] to describe wave scattering by a submerged, circular cylinder. Thus, in the outer region $\phi$ is written as

$$\phi = e^{iKx-Ky} + Ka\sum_{n=1}^{\infty}\frac{a^n}{n}[p_n^s\phi_n^s + p_n^a\phi_n^a] \tag{7}$$

where $\phi_n^s$ and $\phi_n^a$ are the symmetric and antisymmetric multipole potentials given by

$$\phi_n^s = \frac{\cos n\theta}{r^n} + \frac{(-1)^{n-1}}{(n-1)!}\int_0^{\infty}\left[\frac{K+\ell}{K-\ell}\right]\ell^{n-1}e^{-\ell(y+h)}\cos\ell x\,\mathrm{d}\ell + \frac{(-1)^n}{(n-1)!}2\pi iK^n e^{-K(y+h)}\cos Kx \tag{8}$$

and

$$\phi_n^a = \frac{\sin n\theta}{r^n} + \frac{(-1)^n}{(n-1)!}\int_0^{\infty}\left[\frac{K+\ell}{K-\ell}\right]\ell^{n-1}e^{-\ell(y+h)}\sin\ell x\,\mathrm{d}\ell + \frac{(-1)^{n-1}}{(n-1)!}2\pi iK^n e^{-K(y+h)}\sin Kx \tag{9}$$

and $p_n^s$ and $p_n^a$ are coefficients to be determined by appropriate matching of the solution for $\phi$ to that in the inner region. By deforming the contour of integration in equations (8) and (9) it may be shown that

$$\phi_n^s \sim \frac{(-1)^n}{(n-1)!} 2\pi i K^n e^{-Kh} e^{iK|x|-Ky} \quad \text{as } |x| \to \infty \tag{10}$$

and

$$\phi_n^a \sim \frac{(-1)^{n-1}}{(n-1)!} \operatorname{sgn}(x) 2\pi K^n e^{-Kh} e^{iK|x|-Ky} \quad \text{as } |x| \to \infty \tag{11}$$

Thus, the expansion in (7) automatically satisfies the radiation condition (6) provided that the reflection and transmission coefficients are defined by

$$R = 2\pi e^{-Kh} \sum_{n=1}^{\infty} \frac{(-1)^n (Ka)^{n+1}}{n!} (p_n^a + i p_n^s) \tag{12}$$

and

$$T = 1 + 2\pi e^{-Kh} \sum_{n=1}^{\infty} \frac{(-1)^n (Ka)^{n+1}}{n!} (-p_n^a + i p_n^s). \tag{13}$$

In the inner region, $r < a$, there is no free surface and so the potential may be expressed as

$$\phi = e^{iKx-Ky} + A_0 + \sum_{n=1}^{\infty} \frac{r^n}{a^n} [A_n \cos n\theta + B_n \sin n\theta] \tag{14}$$

where $A_n$ and $B_n$ are further coefficients to be determined. (The incident wave term is included in (14) for later convenience. In principle, it could be expanded in a series of $r^n \cos n\theta$ and $r^n \sin n\theta$ and incorporated into the existing series.) The unknown coefficients in (7) and (14) are determined by requiring the potential in each region to satisfy the body boundary condition (4) and also by requiring $\phi$ and $\partial\phi/\partial r$ to be continuous on $r = a$, $-\alpha < \theta < \alpha$ to ensure continuity of pressure and velocity in the fluid. A combination of these conditions shows that $\partial\phi/\partial r$ is continuous everywhere on $r = a$, (except at the actual plate tips where there is a square root singularity in the velocity). Thus, the inner and outer expansions for $\phi$ in (7) and (14) may be differentiated with respect to $r$ and equated on $r = a$. After the multipole potentials are expanded in terms of $\cos m\theta$ and $\sin m\theta$ this yields

$$Ka \sum_{n=1}^{\infty} \left\{ p_n^s \left[ -\cos n\theta + \sum_{m=1}^{\infty} m M_{mn} \cos m\theta \right] + p_n^a \left[ -\sin n\theta + \sum_{m=1}^{\infty} m M_{mn} \sin m\theta \right] \right\}$$

$$= \sum_{n=1}^{\infty} n [A_n \cos n\theta + B_n \sin n\theta], \quad -\pi < \theta \le \pi, \ \theta \ne \pm\alpha, \tag{15}$$

where

$$M_{mn} = \frac{(-1)^{m+n-1} a^{m+n}}{n!\, m!} \int_0^{\infty} \left[ \frac{K+\ell}{K-\ell} \right] \ell^{m+n-1} e^{-2\ell h} \, d\ell$$

$$+ \frac{(-1)^{m+n}}{n!\, m!} 2\pi i (Ka)^{m+n} e^{-2Kh}. \tag{16}$$

Multiplication of (15) by $\cos k\theta$ and integration from $-\pi$ to $\pi$ gives

$$A_k = Ka\left[-\frac{p_k^s}{k} + \sum_{n=1}^{\infty} p_n^s M_{kn}\right], \quad k = 1, \ldots . \tag{17}$$

Similarly, multiplication of (15) by $\sin k\theta$ and integration from $-\pi$ to $\pi$ gives

$$B_k = Ka\left[-\frac{p_k^a}{k} + \sum_{n=1}^{\infty} p_n^a M_{kn}\right], \quad k = 1, \ldots . \tag{18}$$

Equations (17) and (18) represent expressions for the unknown coefficients in the inner expansion of the potential in terms of the coefficients in the outer expansion. Further relations between the sets of coefficients are obtained by requiring continuity of pressure on the fluid interface section of $r = a$ and by satisfying the body boundary condition (4). From (7) and (14), continuity of $\phi$ on $r = a$, $-\alpha < \theta < \alpha$ requires that

$$Ka\sum_{n=1}^{\infty}\left\{p_n^s\left[\frac{\cos n\theta}{n} + \sum_{m=0}^{\infty} M_{mn}\cos m\theta\right] + p_n^a\left[\frac{\sin n\theta}{n} + \sum_{m=1}^{\infty} M_{mn}\sin m\theta\right]\right\}$$
$$= A_0 + \sum_{n=1}^{\infty} A_n \cos n\theta + B_n \sin n\theta, \quad -\alpha < \theta < \alpha. \tag{19}$$

Multiplication of (19) by $\cos k\theta$ and integration over the range $-\alpha < \theta < \alpha$ gives

$$\sum_{n=1}^{\infty} p_n^s\left[\frac{C_{nk}}{n} + \sum_{m=0}^{\infty} M_{mn}C_{mk}\right] = \sum_{n=0}^{\infty}\frac{A_n C_{nk}}{Ka}, \quad k = 0, 1, \ldots . \tag{20}$$

where

$$C_{nk} = \int_{-\alpha}^{\alpha} \cos n\theta \cos k\theta \, d\theta. \tag{21}$$

Similarly, multiplication of (19) by $\sin k\theta$ and integration over the range $-\alpha < \theta < \alpha$ gives

$$\sum_{n=1}^{\infty} p_n^a\left[\frac{S_{nk}}{n} + \sum_{m=1}^{\infty} M_{mn}S_{mk}\right] = \sum_{n=1}^{\infty}\frac{B_n S_{nk}}{Ka}, \quad k = 1, 2, \ldots . \tag{22}$$

where

$$S_{nk} = \int_{-\alpha}^{\alpha} \sin n\theta \sin k\theta \, d\theta. \tag{23}$$

After the expansion for $\phi$ in the outer region in (7) is differentiated, the body boundary condition (4) yields

$$Ka\sum_{n=1}^{\infty}\left\{p_n^s\left[-\cos n\theta + \sum_{m=1}^{\infty} mM_{mn}\cos m\theta\right] + p_n^a\left[-\sin n\theta + \sum_{m=1}^{\infty} mM_{mn}\sin m\theta\right]\right\}$$
$$= -e^{-Kh}\sum_{n=1}^{\infty}\frac{(-1)^n(Ka)^n}{(n-1)!}[\cos n\theta - i\sin n\theta], \quad \alpha < \theta < 2\pi - \alpha, \tag{24}$$

where the normal derivative of the incident wave train has been expanded on $r = a$ in terms of $\cos n\theta$ and $\sin n\theta$. Multiplication of (24) by $\cos k\theta$ and $\sin k\theta$ respectively and integration over the range $\alpha < \theta < 2\pi - \alpha$ gives

$$\sum_{n=1}^{\infty} p_n^s \left[ -D_{nk} + \sum_{m=1}^{\infty} mM_{mn}D_{mk} \right] = -e^{-Kh} \sum_{n=1}^{\infty} \frac{(-1)^n (Ka)^{n-1}}{(n-1)!} D_{nk}, \quad k = 1, 2, \ldots, \tag{25}$$

and

$$\sum_{n=1}^{\infty} p_n^a \left[ -T_{nk} + \sum_{m=1}^{\infty} mM_{mn}T_{mk} \right] = ie^{-Kh} \sum_{n=1}^{\infty} \frac{(-1)^n (Ka)^{n-1}}{(n-1)!} T_{nk}, \quad k = 1, 2, \ldots, \tag{26}$$

where

$$D_{nk} = \int_{\alpha}^{2\pi-\alpha} \cos n\theta \cos k\theta \, \mathrm{d}\theta = \pi\delta_{nk}(1 + \delta_{n0}) - C_{nk} \tag{27}$$

and

$$T_{nk} = \int_{\alpha}^{2\pi-\alpha} \sin n\theta \sin k\theta \, \mathrm{d}\theta = \pi\delta_{nk}(1 - \delta_{n0}) - S_{nk} \tag{28}$$

where $\delta_{nk}$ is the Kronecker delta. The systems of equations in (20) and (25) arise from applying the appropriate boundary conditions over complementary parts of the interval $-\pi < \theta \leq \pi$ and using a Galerkin-type procedure in each part in turn. In order to include the information over the entire range $-\pi < \theta \leq \pi$ these systems should be combined in an additive fashion. However, there is a certain amount of choice in how the equations are combined. Numerical experimentation suggests that simply adding the two systems together does not lead to a system of equations which exhibits good convergence properties when truncated and a combination which has better numerical properties is obtained when $k/2$ times the system in (20) is subtracted from the system in (25). After the coefficients $A_k$, $k = 1, \ldots$ are eliminated from (20) by using (17), this combination of equations yields

$$\sum_{n=1}^{\infty} p_n^s \left\{ C_{nk} \left( 1 - \frac{k}{n} \right) - \delta_{nk}\pi - \frac{k}{2} M_{0n}C_{0k} + \sum_{m=1}^{\infty} mM_{mn}(\delta_{mk}\pi - C_{mk}) \right\}$$

$$- \frac{kC_{0k}}{2Ka} A_0 = e^{-Kh} \sum_{n=1}^{\infty} \frac{(-1)^n (Ka)^{n-1}}{(n-1)!} (C_{nk} - \delta_{nk}\pi), \quad k = 1, \ldots \tag{29}$$

In addition, there is one extra equation which arises from (20) when $k = 0$. After the coefficients $A_k$, $k = 1, \ldots$ have been eliminated this equation becomes

$$\sum_{n=1}^{\infty} p_n^s \left[ \frac{2C_{n0}}{n} + M_{0n}C_{00} \right] - \frac{A_0 C_{00}}{Ka} = 0. \tag{30}$$

In principle, this last equation may be thought of as an equation for $A_0$ in terms of the outer variables, ((17) only holds for $A_k$, $k = 1, \ldots$). In practice, it is more convenient not to eliminate $A_0$ between (30) and (29) but to solve the larger system directly for $p_n^s$ and $A_0$. A similar set of equations are obtained for the antisymmetric multipole coefficients by subtracting $k/2$

times the system in (22) from the system in (26) and eliminating the $B_k$ by using (18). This yields

$$\sum_{n=1}^{\infty} p_n^a \left\{ S_{nk}\left(1-\frac{k}{n}\right) - \delta_{nk}\pi + \sum_{m=1}^{\infty} mM_{mn}(\delta_{mk}\pi - S_{mk}) \right\}$$

$$= ie^{-Kh} \sum_{n=1}^{\infty} \frac{(-1)^n (Ka)^{n-1}}{(n-1)!}(\delta_{nk}\pi - S_{nk}), \quad k = 1, \ldots \tag{31}$$

The systems of equations for the coefficients $p_n^s$, $A_0$ and $p_n^a$ are truncated and solved numerically using a NAG library routine. The resulting coefficients are substituted into the expressions for $R$ and $T$ in (12) and (13) and graphs showing the variation of these quantities with frequency will be presented in §4.

## 3. A variational approximation

In this section, approximations to the reflection and transmission coefficients are obtained using the Schwinger variational procedure. This technique has been applied to many two-dimensional water wave problems involving rectangular geometries by, for example, Miles [19], Mei & Black [17] and Evans & Morris [9]

It is convenient to define $V(\theta)$ to be the jump in potential across the circle $r = a$. This quantity is split into its symmetric and antisymmetric parts, $V(\theta) = V_s(\theta) + V_a(\theta)$ and then expanded on $r = a$ using (14) and (7) to give

$$V_s(\theta) = Ka \sum_{n=1}^{\infty} p_n^s \left[ \frac{\cos n\theta}{n} + \sum_{m=0}^{\infty} M_{mn} \cos m\theta \right] - \sum_{n=0}^{\infty} A_n \cos n\theta, \quad -\pi < \theta \leq \pi \tag{32}$$

and

$$V_a(\theta) = Ka \sum_{n=1}^{\infty} p_n^a \left[ \frac{\sin n\theta}{n} + \sum_{m=1}^{\infty} M_{mn} \sin m\theta \right] - \sum_{n=1}^{\infty} B_n \sin n\theta, \quad -\pi < \theta \leq \pi. \tag{33}$$

The coefficients $A_n$ and $B_n$, $n = 1, \ldots$ are eliminated from (32) and (33) using (17) and (18) to give

$$V_s(\theta) = 2Ka \sum_{n=1}^{\infty} p_n^s \frac{\cos n\theta}{n} - A_0 + Ka \sum_{n=1}^{\infty} p_n^s M_{0n}, \quad -\pi < \theta \leq \pi \tag{34}$$

and

$$V_a(\theta) = 2Ka \sum_{n=1}^{\infty} p_n^a \frac{\sin n\theta}{n}, \quad -\pi < \theta \leq \pi. \tag{35}$$

Multiplication of (34) and (35) by $\cos m\theta$ and $\sin m\theta$ respectively and integration between $-\pi$ and $\pi$ gives

$$\frac{2\pi Ka\, p_m^s}{m} = \int_{\alpha}^{2\pi-\alpha} V_s(\theta) \cos m\theta \, \mathrm{d}\theta, \quad m = 1, \ldots \tag{36}$$

and

$$\frac{2\pi Ka\, p_m^a}{m} = \int_{\alpha}^{2\pi-\alpha} V_a(\theta) \sin m\theta \, \mathrm{d}\theta, \quad m = 1, \ldots, \tag{37}$$

noting that the potential jump on $r = a$ is zero on the fluid interface, i.e. $-\alpha < \theta < \alpha$.

It is also convenient to define $U(\theta)$ by

$$U(\theta) = a\frac{\partial}{\partial r}[\phi - e^{iKx-Ky}] \quad \text{on } r = a,\ -\pi < \theta \leq \pi,\ \theta \neq \pm\alpha. \tag{38}$$

This is split into its symmetric and antisymmetric parts, $U(\theta) = U_s(\theta) + U_a(\theta)$ and from (7) may be written as

$$U_s(\theta) - iKa\sum_{n=1}^{\infty}\sum_{m=1}^{\infty} p_n^s m M_{mn}^i \cos m\theta = Ka\sum_{n=1}^{\infty} p_n^s\left(-\cos n\theta + \sum_{m=1}^{\infty} m M_{mn}^r \cos m\theta\right) \tag{39}$$

and

$$U_a(\theta) - iKa\sum_{n=1}^{\infty}\sum_{m=1}^{\infty} p_n^a m M_{mn}^i \sin m\theta = Ka\sum_{n=1}^{\infty} p_n^a\left(-\sin n\theta + \sum_{m=1}^{\infty} m M_{mn}^r \sin m\theta\right), \tag{40}$$

where $M_{mn}^r$ and $M_{mn}^i$ are the real and imaginary parts of $M_{mn}$ respectively. From the body boundary condition (4) $U_s(\theta)$ and $U_a(\theta)$ are given on $r = a$, $\alpha < \theta < 2\pi - \alpha$ by

$$U_s(\theta) = -e^{-Kh}\sum_{n=1}^{\infty}\frac{(-1)^n(Ka)^n}{(n-1)!}\cos n\theta \quad \text{on } \alpha < \theta < 2\pi - \alpha \tag{41}$$

and

$$U_a(\theta) = ie^{-Kh}\sum_{n=1}^{\infty}\frac{(-1)^n(Ka)^n}{(n-1)!}\sin n\theta \quad \text{on } \alpha < \theta < 2\pi - \alpha. \tag{42}$$

From (12) the reflection coefficient may be written as $R = R_s + R_a$ where

$$R_s = 2\pi i e^{-Kh}\sum_{n=1}^{\infty}\frac{(-1)^n(Ka)^{n+1}}{n!}p_n^s \tag{43}$$

and

$$R_a = 2\pi e^{-Kh}\sum_{n=1}^{\infty}\frac{(-1)^n(Ka)^{n+1}}{n!}p_n^a. \tag{44}$$

This may be used together with (16), (41) and (42) to rewrite the left-hand sides of (39) and (40) as $U_s(\theta)(1 + R_s)$ and $U_a(\theta)(1 - R_a)$ respectively, in the region $\alpha < \theta < 2\pi - \alpha$. Thus, substitution of (36) and (37) into the right-hand sides of (39) and (40) yields

$$U_s(\theta)(1 + R_s) = \sum_{n=1}^{\infty}\int_{\alpha}^{2\pi-\alpha} K_{ns}(\theta, \theta')V_s(\theta')\,\mathrm{d}\theta', \quad \alpha < \theta < 2\pi - \alpha, \tag{45}$$

where

$$K_{ns}(\theta, \theta') = \frac{1}{2\pi}n\left[-\cos n\theta\cos n\theta' + \sum_{m=1}^{\infty} m M_{mn}^r \cos m\theta\cos n\theta'\right] \tag{46}$$

and

$$U_a(\theta)(1 - R_a) = \sum_{n=1}^{\infty} \int_{\alpha}^{2\pi-\alpha} K_{na}(\theta, \theta') V_a(\theta') \, \mathrm{d}\theta', \quad \alpha < \theta < 2\pi - \alpha, \tag{47}$$

where

$$K_{na}(\theta, \theta') = \frac{1}{2\pi} n \left[ -\sin n\theta \sin n\theta' + \sum_{m=1}^{\infty} m M_{mn}^{\tau} \sin m\theta \sin n\theta' \right]. \tag{48}$$

It is not possible to interchange the order of summation and integration in (45) and (47) as the resulting series would not converge. (Evans & Morris [9] overcame a similar problem by introducing an artificial exponential decay factor in the kernel of the equation and taking the limit as the exponent tends to zero. However, it is not necessary that the order of integration and summation should be changed here.) By writing

$$V_s(\theta) = (1 + R_s) X_s(\theta) \tag{49}$$

and

$$V_a(\theta) = i(1 - R_a) X_a(\theta) \tag{50}$$

the following equations are obtained for $X_s$ and $X_a$:

$$\sum_{n=1}^{\infty} \int_{\alpha}^{2\pi-\alpha} K_{ns}(\theta, \theta') X_s(\theta') \, \mathrm{d}\theta' = U_s(\theta), \quad \alpha < \theta < 2\pi - \alpha \tag{51}$$

and

$$\sum_{n=1}^{\infty} \int_{\alpha}^{2\pi-\alpha} K_{na}(\theta, \theta') X_a(\theta') \, \mathrm{d}\theta' = -iU_a(\theta), \quad \alpha < \theta < 2\pi - \alpha. \tag{52}$$

The quantities $K_{ns}(\theta, \theta')$, $K_{na}(\theta, \theta')$, $U_s(\theta)$ and $-iU_a(\theta)$ are all real and so $X_s$ and $X_a$ must be real functions. From (43) and (41) it may be shown that

$$R_s = -i \int_{\alpha}^{2\pi-\alpha} V_s(\theta) U_s(\theta) \, \mathrm{d}\theta \tag{53}$$

and so by rewriting $V_s$ in terms of $X_s$ using (49), $R_s$ may be written as

$$R_s = \frac{Q_s}{i - Q_s} \tag{54}$$

where

$$Q_s = \int_{\alpha}^{2\pi-\alpha} X_s(\theta) U_s(\theta) \, \mathrm{d}\theta \tag{55}$$

and $Q_s$ is a real quantity. A similar analysis gives

$$R_a = \frac{Q_a}{Q_a - i} \tag{56}$$

where

$$Q_a = \int_\alpha^{2\pi-\alpha} X_a(\theta)(-iU_a(\theta))\,\mathrm{d}\theta \tag{57}$$

and $Q_a$ is also a real quantity.

A variational approximation to $X_s$ is sought in the form $X_s(\theta) = a_s W_s(\theta)$ where $a_s$ is a constant and is chosen so that

$$\int_\alpha^{2\pi-\alpha} a_s W_s(\theta) U_s(\theta)\,\mathrm{d}\theta = \int_\alpha^{2\pi-\alpha} a_s W_s(\theta) \sum_{n=1}^{\infty} \int_\alpha^{2\pi-\alpha} K_{ns}(\theta,\theta') a_s W_s(\theta')\,\mathrm{d}\theta'\mathrm{d}\theta. \tag{58}$$

Substitution of this approximation into (55) yields

$$Q_s = \frac{\left[\int_\alpha^{2\pi-\alpha} U_s(\theta) W_s(\theta)\,\mathrm{d}\theta\right]^2}{\int_\alpha^{2\pi-\alpha} W_s(\theta) \sum_{n=1}^{\infty} \int_\alpha^{2\pi-\alpha} K_{ns}(\theta,\theta') W_s(\theta')\,\mathrm{d}\theta'\mathrm{d}\theta}. \tag{59}$$

The success of the approximation depends on a suitable choice for the function $W_s(\theta)$. There are square root singularities in the velocity at the tips of the plates and the simplest way to model this is to choose

$$W_s(\theta) = (\theta-\alpha)^{1/2}(2\pi-\alpha-\theta)^{1/2}, \quad \alpha \le \theta \le 2\pi-\alpha. \tag{60}$$

Such an approximation allows only a very simple variation in potential along the length of the plate and so may be expected to give good results only when the plate is short compared to the wavelength and occupies a small part of the circle. A similar approximation was used by Mei & Petroni [20] when considering the wave scattering by a vertical, circular harbour which contains a narrow gap. Substitution of (60) into (59) yields

$$Q_s = \frac{2\pi e^{-2Kh}\left[\sum_{n=1}^{\infty} \frac{(Ka)^n}{n!} J_1(n(\pi-\alpha))\right]^2}{\sum_{n=1}^{\infty}\left[-\frac{J_1^2(n(\pi-\alpha))}{n} + \sum_{m=1}^{\infty}(-1)^{m+n} M_{mn}^r J_1(n(\pi-\alpha)) J_1(m(\pi-\alpha))\right]}, \tag{61}$$

where Gradshteyn & Ryzhik [21] (3.752.2) has been used to write

$$\int_\alpha^{2\pi-\alpha} \cos n\theta\,(\theta-\alpha)^{1/2}(2\pi-\alpha-\theta)^{1/2}\,\mathrm{d}\theta = \frac{(-1)^n}{n}\pi(\pi-\alpha)J_1(n(\pi-\alpha)) \tag{62}$$

and $J_1$ is a Bessel function of the first kind.

The corresponding variational approximation to $X_a(\theta)$ is given by $X_a(\theta) = a_a W_a(\theta)$ where

$$W_a(\theta) = (\theta-\pi)(\theta-\alpha)^{1/2}(2\pi-\alpha-\theta)^{1/2}, \quad \alpha \le \theta \le 2\pi-\alpha \tag{63}$$

and the constant $a_a$ satisfies

$$\int_\alpha^{2\pi-\alpha} a_a W_a(\theta)(-iU_a(\theta))\,\mathrm{d}\theta = \int_\alpha^{2\pi-\alpha} a_a W_a(\theta) \sum_{n=1}^{\infty} \int_\alpha^{2\pi-\alpha} K_{na}(\theta,\theta') a_a W_a(\theta')\,\mathrm{d}\theta'\mathrm{d}\theta. \tag{64}$$

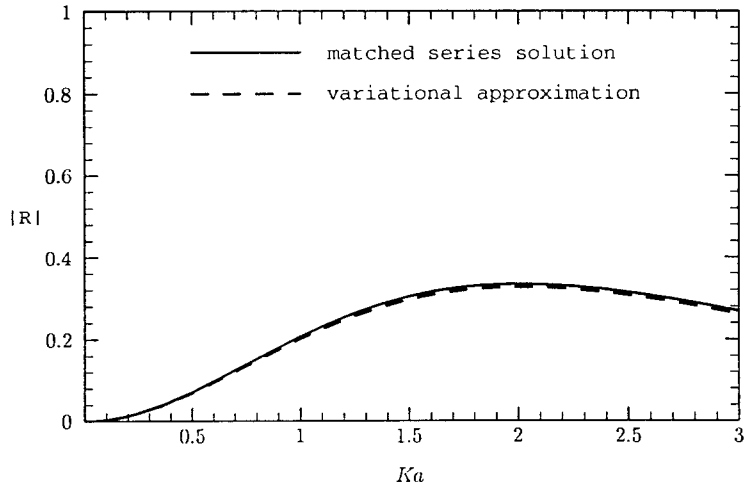


*Fig. 2.* Comparison of approximate and exact values of $|R|$; $a/h = 0.8$, $\alpha = 0.9\pi$

A similar analysis yields

$$Q_a = \frac{2\pi e^{-2Kh}\left[\sum_{n=1}^{\infty}\frac{(Ka)^n}{n!}J_2(n(\pi-\alpha))\right]^2}{\sum_{n=1}^{\infty}\left[-\frac{J_2^2(n(\pi-\alpha))}{n}+\sum_{m=1}^{\infty}(-1)^{m+n}M_{mn}^r J_2(n(\pi-\alpha))J_2(m(\pi-\alpha))\right]} \tag{65}$$

where Gradshteyn & Ryzhik [21] (3.771.10) has been used to write

$$\int_{\alpha}^{2\pi-\alpha}\sin n\theta(\theta-\pi)(\theta-\alpha)^{1/2}(2\pi-\alpha-\theta)^{1/2}\,\mathrm{d}\theta = \frac{(-1)^n}{n}\pi(\pi-\alpha)^2 J_2(n(\pi-\alpha)) \tag{66}$$

and $J_2$ is a Bessel function of the first kind. The expressions for $Q_s$ and $Q_a$ in (61) and (65) are substituted into (54) and (56) and the resulting approximation to the reflection coefficient is compared with the results from the full numerical solution in the next section.

## 4. Results and discussion

The numerical scheme for the matched series expansion method, described in §2, was first checked by reproducing the results of Ursell [16] for the submerged, circular cylinder in the limit as $\alpha \to 0$ and also ensuring that energy was conserved, (i.e. $|R|^2 + |T|^2 = 1$). Values of the reflection coefficient were then compared with those given by Parsons & Martin [15] for a number of different plates and two decimal place agreement was obtained in the majority of cases as demonstrated in Table 1. In all the calculations, it was found that 256 multipole potentials were sufficient to ensure numerical results accurate to two decimal places and in several cases less terms were required. In particular, many fewer terms were needed to model the wave scattering by a circular cylinder than any one of the plates. This is thought to be because the velocity potential is modelled by a series of smooth functions and in order to produce a singularity in its derivative at the tips of the plate, the coefficients in the series have to decay at a certain rate which is not as fast as the coefficients in a series for which the velocity is bounded. Thus more terms are needed in the series expansion to obtain the same

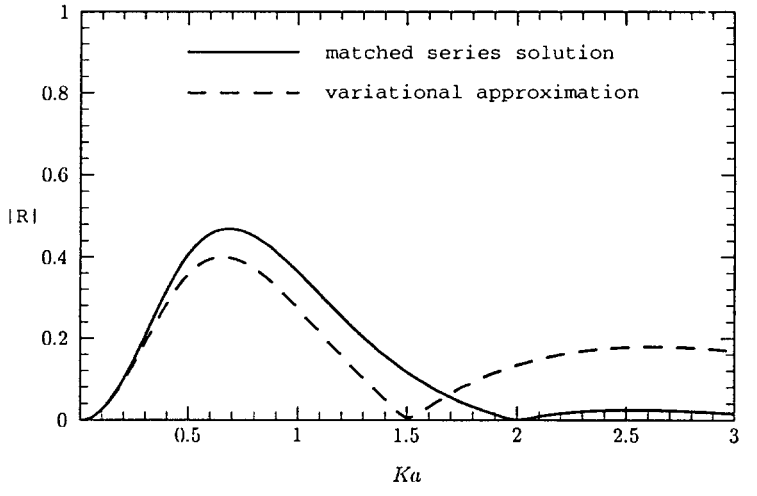


*Fig. 3.* Comparison of approximate and exact values of $|R|$; $a/h = 0.8$, $\alpha = 0.7\pi$

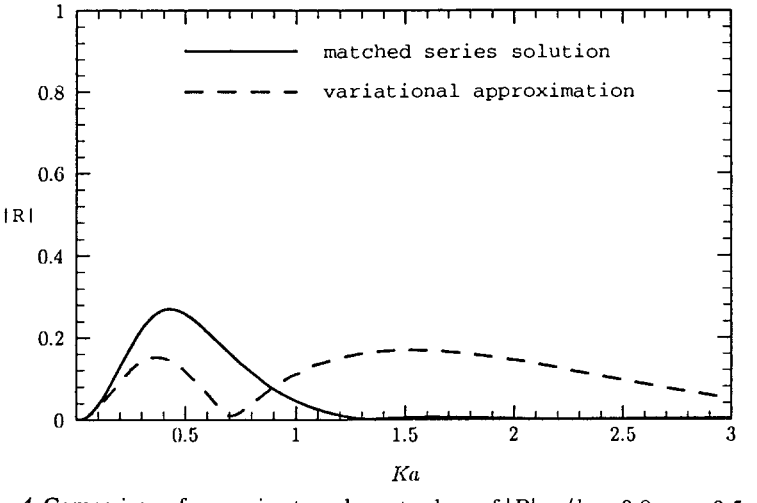


*Fig. 4.* Comparison of approximate and exact values of $|R|$; $a/h = 0.8$, $\alpha = 0.5\pi$

level of accuracy in any calculation. Here the variational approximation has an advantage over the full solution as the behaviour of the potential at the ends of the plate appeared explicitly in its representation, as shown in (60) and (63). The disadvantage of the approximation is that it does not allow for large variations in the potential along the length of the plate and so is expected to perform well only when the plate is short compared to the wavelength and occupies a small fraction of a circle. Analogous results were obtained by Mei & Petroni [20] who used a similar approximation when modelling the wave scattering by a vertical, circular harbour which contains a narrow gap.

Figures 2–4 compare the values of $|R|$ calculated from the full numerical solution with those obtained from the variational approximation for plates for which $a/h = 0.8$. The first of these figures is for a plate of length equal to $0.2\pi a$, (equivalent to a value of $\alpha = 0.9\pi$). This is the shortest of the three plates and so is the one for which the approximate solution should give the best agreement. As can be clearly seen from figure 2, the approximation to the reflection

*Table 1.* Comparison of the matched series results with results of Parsons & Martin [15]

| Plate parameters | $Ka$ | Matched series results $\lvert R\rvert$ | arg $R$ | Parsons & Martin [15] $\lvert R\rvert$ | arg $R$ |
|---|---|---|---|---|---|
| $a/h = 0.9139$ | 0.5305 | 0.7223 | 2.8094 | 0.7237 | 2.7998 |
| $\alpha = 0.7\pi$ | 1.0610 | 0.2743 | -2.3145 | 0.2852 | -2.3264 |
| | 1.5915 | 0.0518 | 1.1029 | 0.0506 | 1.0992 |
| | 2.1221 | 0.0485 | 1.0874 | 0.0507 | 1.0845 |
| $a/h = 0.8884$ | 0.3979 | 0.4820 | 2.5410 | 0.4841 | 2.5352 |
| $\alpha = 0.6\pi$ | 0.7958 | 0.2586 | -2.6607 | 0.2648 | -2.6675 |
| | 1.1937 | 0.0083 | -2.3713 | 0.0097 | -2.3738 |
| | 1.5915 | 0.0277 | 0.7732 | 0.0283 | 0.7718 |
| $a/h = 0.8642$ | 0.3183 | 0.2935 | 2.3490 | 0.2957 | 2.3460 |
| $\alpha = 0.5\pi$ | 0.6366 | 0.2057 | -2.9432 | 0.2095 | -2.9466 |
| | 0.9549 | 0.0353 | -2.6399 | 0.0364 | -2.6408 |
| | 1.2732 | 0.0083 | 0.5278 | 0.0084 | 0.5278 |

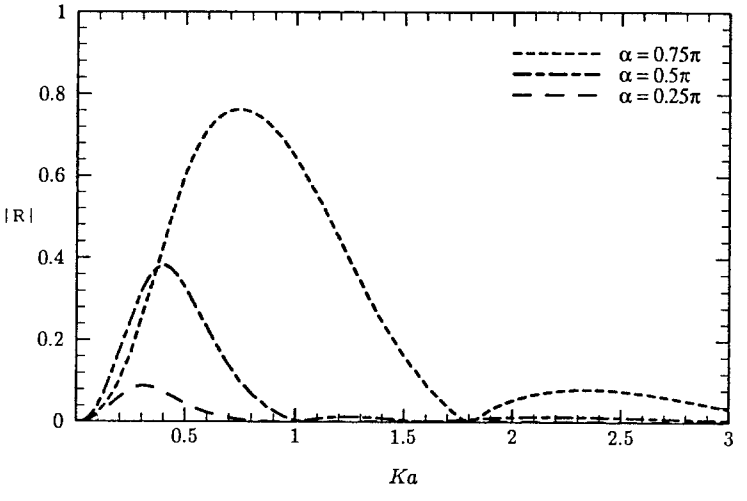


*Fig. 5.* Variation of $|R|$ with frequency; $a/h = 0.9$

coefficient is very close to the exact solution over the whole range of frequencies considered. The next largest plate has a length equal to $0.6\pi a$, (equivalent of a value of $\alpha = 0.7\pi$). From figure 3 it may be observed that whilst the approximation is good at low frequencies, it starts to diverge from the true solution at $Ka \approx 0.4$. It is often possible to prove that quantities calculated using a variational procedure provide bounds for the exact quantities, (see e.g. Evans & Morris [9]). In this case, the numerical evidence indicates that the values of $Q_s$ and $Q_a$ generated from the variational approximation are negative and, in magnitude, are lower bounds for the exact values. However, we were unable to prove this because we were unable to show that the operators in (51) and (52) are negative definite. Even if the variational approximation does yield bounds for $Q_s$ and $Q_a$ these do not translate a bound for

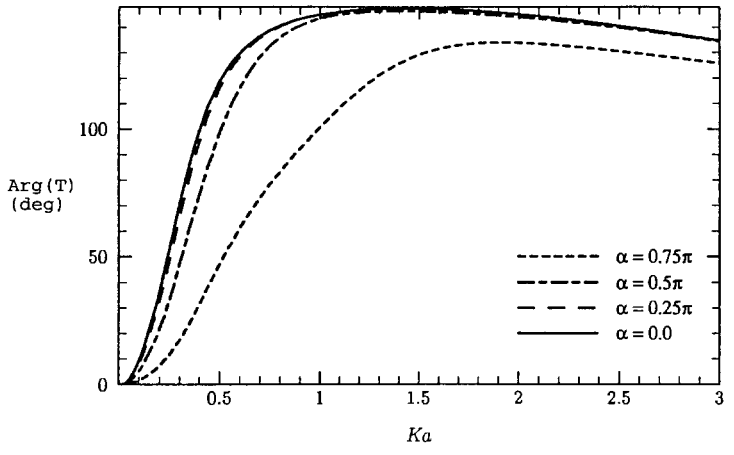


*Fig. 6.* Variation of Arg($T$) with frequency; $a/h = 0.9$

the total reflection coefficient because of the way it is constructed from $Q_s$ and $Q_a$. This is apparent in Fig. 3 where the approximate solution sometimes underestimates and sometimes overestimates the magnitude of the reflection coefficient. Fig. 4 compares the approximate and full solution for a semi-circular plate. In this case, the approximation is not particularly good except at very low frequencies and for plates of this length or longer it would be desirable to seek other approximations such as those based on high or low frequency asymptotics or even small gap approximations.

The main purpose of this work is to see how the reflection and transmission properties of circular arc plates compare with those for the corresponding circular cylinder and thus assess the suitability of the arc plate as a lens element. Figure 5 illustrates the variation of the reflection coefficient with frequency for a set of plates of different lengths at a depth of $a/h = 0.9$. The matched series expansion method has been used for these calculations. The corresponding reflection coefficient for the circular cylinder is of course zero for all frequencies. As expected, as $\alpha$ decreases and the plate occupies more of the circle, so the reflection coefficient decreases on average. In particular, for plates which occupy half a circle or more there is very little reflection. However, for the shortest plate with a value of $\alpha = 0.75\pi$ there can be substantial amounts of reflection at low frequencies. Figure 6 illustrates the variation in the phase of the transmission coefficient with frequency for the same set of plates. In addition, the results for the corresponding circular cylinder are given. Again the variation in the phase of the transmission coefficient does not significantly depend on the position of the ends of the plate for plates which occupy half a circle or more. It is as if the wave field only 'sees' the top part of the body and the fact that the lower part of the cylinder is missing has an insignificant effect. Thus, in circumstances in which the circular cylinder produces suitable phase shifts to be used as a lens element, a circular arc plate occupying a least half of the same circle should also be a candidate. The differences in the phase of the transmission coefficient are more noticeable when comparing the shortest plate with the cylinder, particularly at low frequencies. For these shorter plates, it is probably more sensible to compare the results with those for a submerged horizontal plate rather than those for a submerged circular cylinder.

## 5. Conclusion

In this work, the wave scattering by a circular arc plate submerged in deep water has been investigated using linear theory. A full numerical expression for the velocity potential was

obtained using multipole potentials and a matching procedure. In addition, an explicit approximate solution which modelled exactly the behaviour of the velocity potential at the tips of the plate was derived using a variational procedure. The approximation to the reflection coefficient proved to be accurate for plates which were short compared with the wavelength and occupied a small part of a circle. The full numerical solution was used to compare the reflection and transmission coefficients associated with a number of plates with the corresponding coefficients for a submerged circular cylinder and it was found that there was very little difference between the reflective properties of plates which occupy a half circle or more and those of a circular cylinder.

## Acknowledgements

The authors would like to thank Dr David Porter for helpful advice about integral equations.

## References

1. E. Mehlum and J. J. Stamnes, On the focusing of ocean swells and its significance in Power Production, *Central Institute for Industrial Research, Blindern, Oslo, SI Rep* 78 04 08-3 (1978).
2. S. Murashige and T. Kinoshita, An ideal ocean wave focusing lens and its shape. *Applied Ocean Research*, Vol. 14, No. 5, (1992) pp 275-290.
3. E. Mehlum, A circular cylinder in water waves, *Applied Ocean Research*, Vol. 2, No. 4, (1980) pp. 171-177.
4. W. R. Dean, On the reflexion of surface waves by a submerged circular cylinder, *Proc. Camb. Phil. Soc.*, Vol. 44, (1948) pp. 483 - 491.
5. M. McIver, Diffraction of water waves by a moored, horizontal flat plate, *J. Engineering Maths*, Vol. 19, (1985) pp 297 - 319.
6. F. Ursell, The effect of a fixed, vertical barrier on surface waves in deep water, *Proc. Camb. Phil. Soc.*, Vol. 43, (1947) pp. 374 - 382.
7. F. John, Waves in the presence of an inclined barrier, *Comm. Pure. Appl. Maths.*, Vol. 1, (1948) pp. 149 - 200
8. D. V. Evans, Diffraction of water waves by a submerged vertical plate, *J. Fluid Mechanics*, Vol. 40, (1970) pp 433 - 451.
9. D. V. Evans and C. A. N. Morris, The effect of a fixed vertical barrier on obliquely incident surface waves in deep water, *J. Inst. Maths Applics.*, Vol. 9, (1972) pp. 198 - 204.
10. D. Porter, The radiation and scattering of surface waves by vertical barriers, *J. Fluid Mechanics*, Vol. 63, Part 4, (1974) pp. 625 - 634.
11. M. Patarapanich, Maximum and zero reflection from a submerged plate, *J. Waterway, Port, Coastal and Ocean Engineering*, Vol. 110, No. 2, (1984) pp. 171 - 181.
12. J. E. Burke, Scattering of surface waves on an infinitely deep fluid, *J. Mathematical Physics*, Vol. 5, (1964) pp 805 - 819.
13. A. E. Heins, Water waves over a channel of finite depth with a submerged plane barrier, *Canadian J. Maths*, Vol. 2, (1950) pp 210 - 222
14. N. F. Parsons and P.A. Martin, Scattering of water waves by submerged plates using hypersingular integral equations, *Applied Ocean Research*, Vol. 14, (1992) pp. 313 - 321.
15. N. F. Parsons and P. A. Martin, Scattering of water waves by submerged curved plates and by surface-piercing flat plates, *Applied Ocean Research*, Vol 16, (1994) pp. 129 - 139
16. F. Ursell, Surface waves on deep water in the presence of a submerged cylinder. Part I, *Proc. Camb. Phil. Soc.*, Vol. 46, (1950) pp. 141 - 152.
17. C. C. Mei and J. L. Black, Scattering of surface waves by rectangular obstacles in water of finite depth, *J. Fluid Mechanics*, Vol. 38, Part 3, (1969) pp. 499 - 511.
18. A. Norris and Y. Yang, Dynamic stress on a partially bonded fiber, *J. Appl. Mech.*, Vol. 58, (1991) pp. 404 - 409.
19. J. W. Miles, Surface-wave scattering matrix for a shelf, *J. Fluid Mechanics*, Vol. 28, Part 4, (1967) pp. 755 - 767
20. C. C. Mei and R. P. Petroni, Waves in a harbor with protruding breakwaters *J. Waterways, Harbors, Coastal Eng. Proc. ASCE*, Vol. 99, (1973) pp 209 - 229.
21. I. S. Gradshteyn and I. M. Ryzhik, *Tables of Integrals, Series and Products*, Academic Press, New York (1980).